Thermochemistry Is Not a Lower Bound to the Activation Energy of Endothermic Reactions: A Kinetic Study of the Gas-Phase Reaction of Atomic Chlorine with Ammonia†

Yide Gao,‡ I. M. Alecu,‡ P-C. Hsieh,‡ Brad P. Morgan,§ Paul Marshall,*,‡ and Lev N. Krasnoperov||

Department of Chemistry, University of North Texas, P. O. Box 305070, Denton, Texas 76203-5070, Department of Physical Sciences, Morehead State University, 123 Lappin Hall, Morehead, Kentucky 40351, and Department of Chemistry and Environmental Science, New Jersey Institute of Technology, Newark, New Jersey 07102

Received: November 6, 2005

The rate constant for $Cl + NH_3 \rightarrow HCl + NH_2$ has been measured over 290−570 K by the time-resolved resonance fluorescence technique. Ground-state Cl atoms were generated by 193 nm excimer laser photolysis of CCl_4 and reacted under pseudo-first-order conditions with excess NH_3. The forward rate constant was fit by the expression $k_1 = (1.08 \pm 0.05) \times 10^{-11} \exp(-11.47 \pm 0.16 \text{ kJ mol}^{-1}/RT)$ cm^3 molecule^{-1} s^{-1}, where the uncertainties in the Arrhenius parameters are $\pm 1\ \sigma$ and the 95% confidence limits for k_1 are ±11%. To rationalize the activation energy, which is 7.4 kJ mol^{-1} below the endothermicity in the middle of the $1/T$ range, the potential energy surface was characterized with MPWB1K/6-31++G(2df,2p) theory. The products $NH_2 + HCl$ form a hydrogen-bonded adduct, separated from $Cl + NH_3$ by a transition state lower in energy than the products. The rate constant for the reverse process k_{-1} was derived via modified transition state theory, and the computed k_{-1} exhibits a negative activation energy, which in combination with the experimental equilibrium constant yields k_1 in fair accord with experiment.

1. Introduction

A standard assumption is that, for an endothermic gas-phase reaction of the kind A + B → C + D, a lower bound to the activation energy E_a for the rate constant k is set by the overall enthalpy change $\Delta H°$.[1,2] That is, $E_a = -R\ \mathrm{d}(\ln k)/\mathrm{d}(1/T) \geq \Delta H°$. However, the phenomenon of negative activation energies for apparently elementary gas-phase reactions is now well-known.[3−6] Some of these have been interpreted in terms of formation of an intermediate bound complex in the entrance channel, followed by a tight transition state (TS) whose energy lies below that of the reactants.[7−9] Because the overall reaction enthalpy equals the difference between the activation energies for the forward and reverse reactions,[10] a consequence is that the activation energy for the reverse of a process with a negative temperature dependence is less than its endothermicity. This may be important in cases where the observed E_a is used to set an upper limit to $\Delta H°$, or in estimation of upper limits to rate constants where an assumed preexponential factor is combined with an E_a equal to $\Delta H°$. There is little information in the literature concerning the validity of the assumption $E_a \geq \Delta H°$ for this kind of reaction where complexes might be involved in the exit channel. Here, we present the first determination of the temperature dependence of the rate constant k_1 for the endothermic reaction

$$Cl + NH_3 \rightarrow HCl + NH_2 \qquad (1)$$

and compare it with the isoelectronic and also endothermic reaction

$$Cl + CH_4 \rightarrow HCl + CH_3 \qquad (2)$$

As will be seen, E_a is significantly below $\Delta H°$ for reaction 1, while E_a exceeds $\Delta H°$ for reaction 2. An important difference between the two reactions is that strong hydrogen bonding is only possible between the products of reaction 1. This stabilizes the TS and leads to a negative E_a for the reverse of reaction 1. A computational investigation of the potential energy surface (PES) confirms that the TS is followed by a hydrogen-bonded complex between HCl and NH_2, and this PES is analyzed via transition-state theory for quantitative comparison with the measurements.

2. Experimental Technique

Details of the apparatus and its operation have been given previously.[11,12] Briefly, ground-state atomic chlorine was produced by 193-nm excimer laser (MPB PSX-100, beam cross-section 7 × 8 mm^2) photolysis of CCl_4 precursor and monitored by time-resolved resonance fluorescence at 134−140 nm ($(4s)^2P \rightarrow (4p)^2P_{1/2,3/2}$).[13] This fluorescence was excited by a microwave discharge through a separate flow of Cl_2 (0.2% in Ar, 0.2 mbar pressure). The experiments were conducted in a large excess of Ar bath gas to thermalize the system and to slow diffusion of Cl to the reactor walls. Low photolysis energies F were employed, to minimize secondary chemistry involving photolysis or chemical products. Above 570 K, so many H atoms were produced from NH_3 photolysis that their fluorescence, excited by trace hydrogen impurities in the resonance lamp, interfered, despite the use of calcium fluoride optics. The initial atom concentration $[Cl]_0$ was estimated from the laser fluence and the room-temperature absorption cross-section of CCl_4.[14] It does

† Part of the special issue "David M. Golden Festschrift".
* Corresponding author: marshall@unt.edu.
‡ University of North Texas.
§ Morehead State University.
|| New Jersey Institute of Technology.

10.1021/jp056406l CCC: $33.50
Published on Web 03/09/2006

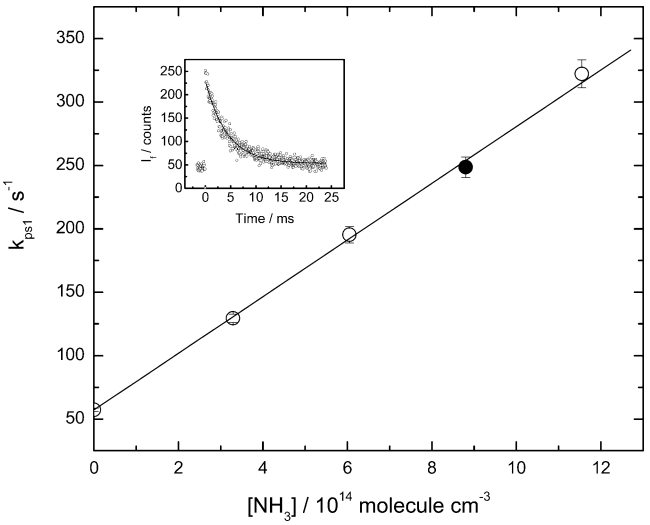

Figure 1. Plot of k_{ps1} vs [NH_3] obtained at 357 K. The error bars are 1 σ. The inset shows the fluorescence signal plus background corresponding to the filled point.

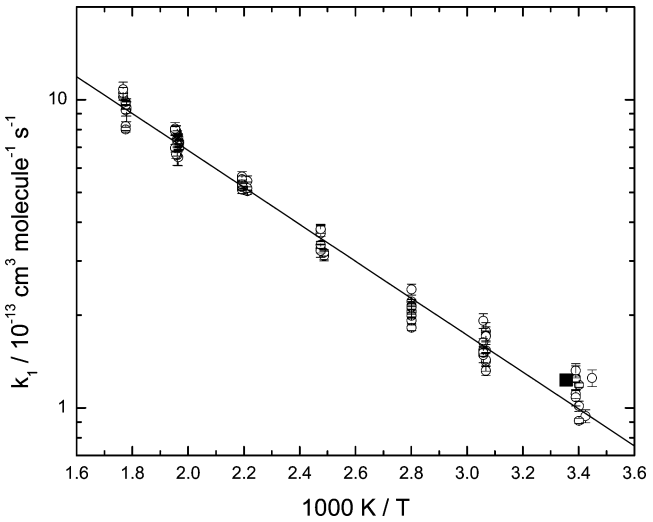

Figure 2. Arrhenius plot for Cl + NH_3. Open circles, present measurements with 1 σ statistical error bars; solid square, measurement by Westenberg and deHaas.[15]

not need to be known for the kinetic analysis, but verifies that the pseudo-first-order condition $[Cl]_0 \ll [NH_3]$ was attained. The ammonia concentration is effectively constant, so that

$$d[Cl]/dt = -k_1[NH_3][Cl] - k'[Cl] = -k_{ps1}[Cl] \quad (3)$$

and exponential decays of the fluorescence signal were obtained. An example is shown in Figure 1. Nonlinear least-squares fitting provided the first-order decay coefficient k_{ps1}, and plots of k_{ps1} vs [NH_3], such as that shown in Figure 1, have slopes equal to k_1. Typically, five values of [NH_3] were employed at each set of conditions, from zero to $[NH_3]_{max}$. The intercept k' arises from diffusional loss of Cl and any reaction with photolysis fragments of CCl_4 and NH_3. The experimental parameters pressure p, $[Cl]_0$, F, and the residence time of gases in the heated reactor τ_{res} were varied to check for any influence on the measured k_1 values.

3. Results and Discussion

Eighty-three measurements over 290−570 K are summarized in Table 1. It may be seen that there is no systematic variation of k_1 with p, $[Cl]_0$, F, and τ_{res}, which indicates that the reaction is effectively bimolecular, has been successfully isolated from any secondary chemistry, and is unaffected by decomposition of the reactants inside the heated reaction cell. Potential interference might arise from condensation of HCl product with NH_3 to form solid NH_4Cl, but no obvious light scattering problems were encountered. The kinetic data are plotted in Arrhenius form in Figure 2. A weighted linear fit was based on the 1 σ uncertainties in the slopes of plots such as Figure 1, listed in Table 1, combined with an estimated $\sigma_T/T = 2\%$, and yielded

$$k_1 = (1.08 \pm 0.05) \times 10^{-11} \exp(-11.47 \pm 0.16 \text{ kJ mol}^{-1}/RT) \text{ cm}^3 \text{ molecule}^{-1} \text{ s}^{-1} \quad (4)$$

where the uncertainties in the Arrhenius parameters are ±1 σ. Together with the covariance and a 10% allowance for potential systematic errors, these yield 95% confidence limits of ±11% for k_1. The only prior measurement of reaction 1 was made by Westenberg and DeHaas with flash lamp photolysis of the same CCl_4 precursor, and they obtained (1.23 ± 0.02) × 10^{-13} cm^3 molecule^{-1} s^{-1} at room temperature.[15] As may be seen from Figure 2, this earlier result lies in the range of our measurements.

Figure 2 also shows that most of the measurements at room temperature lie slightly above the linear Arrhenius fit. This could indicate slight curvature in the Arrhenius plot or that a second channel becomes important at low temperatures. A possible adduct is discussed in the next section. However, we note that there is no systematic pressure influence on the room-temperature data, over a variation of more than a factor of 5. This is evidence against an addition pathway, which would be expected to be pressure-dependent. If such a path was at its high-pressure limit under our conditions, then rate constants of around 10^{-10} cm^3 molecule^{-1} s^{-1} would be expected. Most likely, the adduct is thermodynamically unstable, as discussed in the following section.

The thermochemistry of reaction 1 is well-established. The spectroscopic measurements of Mordaunt et al. yield a precise bond strength for ammonia of 444.0 ± 0.2 kJ mol^{-1} at 0 K,[16] and the bond strength of HCl from Gurvich et al. is 427.8 ± 0.1 kJ mol^{-1}.[17] The difference is $\Delta H_0^\circ = 16.2 \pm 0.2$ kJ mol^{-1}, and via tabulated temperature dependences of the enthalpies,[17] at the approximate center of the T^{-1} range, $\Delta H_{400}^\circ = 18.9$ kJ mol^{-1}, significantly larger than the measured activation energy. Because, as noted in the Introduction, $\Delta H^\circ = E_a(k_1) - E_a(k_{-1})$,[10] the activation energy of the reverse process must be negative.

Reaction 1 can be compared with the isoelectronic reaction 2. The measured variation of k_2 with temperature yields a curved Arrhenius plot,[18] and near the middle of the same temperature range as here yields average Arrhenius parameters of about $A = 1.9 \times 10^{-11}$ cm^3 molecule^{-1} s^{-1} and $E_a = 13.1$ kJ mol^{-1}. These parameters and the corresponding k_2 values are similar to those determined here. The activation energy for reaction 2 is slightly larger than for 1, but by contrast to the latter case, it exceeds the endothermicity, where for reaction 2, $\Delta H_{298}^\circ = 7.5 \pm 0.3$ kJ mol^{-1} and $\Delta H_{400}^\circ = 8.4 \pm 0.3$ kJ mol^{-1}.[17,19,20] Quantitative analysis of reaction 2 includes no role for bound intermediates,[21] and we would expect no strong interaction between CH_3 and HCl. Their reaction, the reverse of reaction 2, has a positive temperature dependence.[22] The electronegativity of nitrogen makes hydrogen bonding feasible between NH_2 and HCl, which, apart from leading to a bound intermediate, also stabilizes the transition state for the reaction. This idea, and

TABLE 1: Summary of Measurements of the Rate Constant k_1 for Cl + NH_3

T K	τ_{res} s	F mJ	p mbar	$[CCl_4]$ 10^{15} molecule cm^{-3}	$[NH_3]_{max}$ 10^{15} molecule cm^{-3}	$[Cl]_0$ 10^{12} molecule cm^{-3}	$k_1 \pm \sigma_{k1}$ 10^{-13} cm^3 molecule^{-1} s^{-1}
290	1.2	0.41	28	2.72	3.47	0.9	1.25 ± 0.08
292	0.9	0.18	43	1.80	1.51	0.3	0.94 ± 0.05
294	2.2	0.21	49	4.05	1.27	0.7	0.91 ± 0.02
294	6.9	0.20	147	5.54	2.05	0.9	1.19 ± 0.02
294	1.6	0.11	36	3.77	1.48	0.3	1.01 ± 0.04
295	4.9	0.15	155	5.45	3.09	0.7	1.25 ± 0.12
295	3.6	0.30	80	5.93	2.19	1.5	1.32 ± 0.07
295	3.6	0.19	80	5.93	2.19	0.9	1.11 ± 0.04
295	3.4	0.14	76	5.64	1.42	0.6	1.24 ± 0.03
295	3.5	0.09	79	5.94	1.24	0.4	1.08 ± 0.07
326	1.4	0.79	35	2.09	1.31	1.4	1.77 ± 0.12
326	1.4	0.59	35	2.09	1.31	1.0	1.72 ± 0.11
326	1.4	0.36	35	2.09	1.31	0.6	1.41 ± 0.10
326	1.4	0.25	35	2.09	1.31	0.4	1.32 ± 0.05
326	1.6	0.59	71	2.32	1.46	1.1	1.71 ± 0.07
326	1.6	0.35	71	2.32	1.46	0.7	1.54 ± 0.03
326	1.6	0.25	71	2.32	1.46	0.5	1.43 ± 0.07
327	3.0	0.49	73	2.90	1.56	1.2	1.92 ± 0.10
327	3.0	0.29	73	2.90	1.56	0.7	1.63 ± 0.05
327	3.0	0.19	73	2.90	1.56	0.5	1.48 ± 0.08
327	2.3	0.29	148	2.75	1.16	0.7	1.54 ± 0.04
327	2.3	0.19	148	2.75	1.16	0.4	1.51 ± 0.04
357	2.7	0.49	72	2.59	1.13	1.1	2.04 ± 0.09
357	2.7	0.29	72	2.59	1.13	0.6	1.82 ± 0.04
357	2.7	0.19	72	2.59	1.13	0.4	1.92 ± 0.04
357	1.4	0.69	72	2.91	1.16	1.7	2.42 ± 0.10
357	1.4	0.44	72	2.91	1.16	1.1	2.21 ± 0.03
357	1.4	0.29	72	2.91	1.16	0.7	2.06 ± 0.03
357	2.1	0.44	148	2.51	1.25	0.9	2.12 ± 0.04
357	2.1	0.29	148	2.51	1.25	0.6	1.99 ± 0.02
357	1.3	0.69	36	2.34	1.13	1.3	2.15 ± 0.11
357	1.3	0.44	36	2.34	1.13	0.9	2.14 ± 0.10
357	1.3	0.29	36	2.34	1.13	0.6	2.13 ± 0.09
402	0.7	0.62	59	1.69	1.73	0.9	3.14 ± 0.11
402	0.7	0.39	59	1.69	1.73	0.6	3.11 ± 0.11
402	0.7	0.19	59	1.69	1.73	0.3	3.19 ± 0.08
404	1.3	0.65	61	2.01	1.18	1.1	3.77 ± 0.17
404	1.3	0.50	61	2.01	1.18	0.8	3.68 ± 0.21
404	1.3	0.20	61	2.01	1.18	0.3	3.80 ± 0.12
404	0.6	0.60	29	1.53	1.57	0.8	3.29 ± 0.11
404	0.6	0.42	29	1.53	1.57	0.5	3.23 ± 0.15
404	0.6	0.18	29	1.53	1.57	0.2	3.38 ± 0.09
452	0.6	0.79	59	1.46	1.22	1.0	5.05 ± 0.04
452	0.6	0.58	59	1.46	1.22	0.7	5.44 ± 0.22
452	0.6	0.24	59	1.46	1.22	0.3	5.16 ± 0.24
456	0.5	0.63	29	1.61	1.13	0.8	5.41 ± 0.24
456	0.5	0.45	29	1.61	1.13	0.6	5.63 ± 0.21
456	0.5	0.28	29	1.61	1.13	0.4	5.52 ± 0.13
456	1.1	0.73	57	1.65	1.21	1.0	5.10 ± 0.14
456	1.1	0.54	57	1.65	1.21	0.7	5.21 ± 0.13
456	1.1	0.26	57	1.65	1.21	0.4	5.31 ± 0.18
508	0.5	0.34	57	1.27	1.50	0.4	6.97 ± 0.06
508	0.5	0.23	57	1.27	1.50	0.2	7.26 ± 0.13
509	0.9	0.69	71	1.76	1.29	1.0	6.50 ± 0.40
509	0.9	0.37	71	1.76	1.29	0.5	7.24 ± 0.38
509	0.9	0.24	71	1.76	1.29	0.4	7.46 ± 0.26
509	0.9	0.18	71	1.76	1.29	0.3	7.54 ± 0.21
510	0.3	0.43	22	0.98	1.86	0.4	6.60 ± 0.47
510	0.3	0.20	22	0.98	1.86	0.2	7.09 ± 0.52
510	0.6	0.36	45	1.38	1.95	0.4	6.74 ± 0.62
510	0.6	0.17	45	1.38	1.95	0.2	7.47 ± 0.28
510	0.6	0.83	44	1.32	1.69	0.9	7.33 ± 0.35
510	0.6	0.34	44	1.32	1.69	0.4	7.13 ± 0.32
510	0.6	0.16	44	1.32	1.69	0.2	7.75 ± 0.18
511	0.5	0.64	30	1.22	1.45	0.7	6.64 ± 0.19
511	0.5	0.51	30	1.22	1.45	0.5	6.98 ± 0.20
511	0.5	0.28	30	1.22	1.45	0.3	7.85 ± 0.39
511	0.8	0.41	63	2.02	1.31	0.7	7.94 ± 0.27
512	1.0	0.59	59	1.54	2.12	0.8	6.96 ± 0.20
512	1.0	0.25	59	1.54	2.12	0.3	7.91 ± 0.26
512	1.0	0.17	59	1.54	2.12	0.2	8.05 ± 0.37
562	0.5	0.67	45	1.42	1.73	0.8	9.28 ± 0.79

TABLE 1 (Continued)

T K	τ_{res} s	F mJ	p mbar	$[CCl_4]$ 10^{15} molecule cm^{-3}	$[NH_3]_{max}$ 10^{15} molecule cm^{-3}	$[Cl]_0$ 10^{12} molecule cm^{-3}	$k_1 \pm \sigma_{k1}$ 10^{-13} cm^3 molecule^{-1} s^{-1}
562	0.5	0.44	45	1.42	1.73	0.5	9.36 ± 0.51
562	0.5	0.22	45	1.42	1.73	0.3	9.43 ± 0.40
563	0.5	0.59	22	1.35	1.47	0.7	8.21 ± 0.27
563	0.5	0.37	22	1.35	1.47	0.4	9.24 ± 0.40
563	0.5	0.27	22	1.35	1.47	0.3	9.66 ± 0.32
563	0.9	0.76	44	1.84	1.48	1.2	8.00 ± 0.14
563	0.9	0.38	44	1.84	1.48	0.6	9.61 ± 0.31
563	0.9	0.24	44	1.84	1.48	0.4	9.83 ± 0.24
566	0.5	0.61	43	1.85	1.06	0.9	10.20 ± 0.27
566	0.5	0.39	43	1.85	1.06	0.6	10.50 ± 0.45
566	0.5	0.19	43	1.85	1.06	0.3	10.80 ± 0.61

TABLE 2: Enthalpies at 0 K of Stationary Points on the Potential Energy Surface Relative to Cl + NH_3, Derived by Various Methods

method	NH_2 + HCl	Cl−NH_3 2c-3e adduct	transition state	H_2N−HCl intermediate
CBS-QB3	15.1	−40.3	9.4	−1.7
G3B3	14.0	−36.6	11.2	−1.9
MPWB1K/6-31+G(d,p)	26.2	−52.5	12.8	1.5
MPWB1K/6-31+G(2d,p)	19.0	−50.2	9.8	−0.3
MPWB1K/6-31++G(2d,2p)	17.5	−49.1	8.1	−1.6
MPWB1K/6-31+G(2df,2p)	17.2	−47.7	9.0	−1.3
MPWB1K/6-31++G(2df,2p)	17.0	−47.7	8.8	−1.4
MPWB1K/6-311+G(d,p)	20.9	−51.3	9.0	−2.2
MPWB1K/6-311++G(2df,2p)	15.1	−48.3	7.3	−1.9
MPWB1K/6-311++G(3d2f,2df,2p)	14.6	−47.2	8.4	−2.5
experiment	16.2 ± 0.1			

the prediction of a negative activation energy for k_{-1}, is explored quantitatively in the next section.

4. Theoretical Analysis

The *Gaussian 03* program suite[23] was employed to calculate geometries, vibrational frequencies, and energies of stationary points on the PES. Several approaches were used. The composite G3B3 and CBS-QB3 ab initio methodologies were applied[24,25] and also the MPWB1K density functional developed by Zhao and Truhlar for systems involving hydrogen bonding and reaction barriers.[26] These DFT calculations were applied with a variety of basis sets, and the vibrational frequencies were scaled by a factor of 0.955.[26] G3 theory includes a spin−orbit correction of −3.5 kJ mol^{-1} to the energy of atomic Cl, and this correction was applied to the other levels of theory. Spin contamination was negligible, with $\langle S^2 \rangle$ spin expectation values for the open-shell species of at most 0.757, cf. the ideal value of exactly 0.75. Table 2 summarizes the results.

The two composite ab initio approaches are in good accord with the overall reaction enthalpy, although they underestimate ΔH_0° by up to 2 kJ mol^{-1} (which is within their target accuracies). The DFT results show systematic variation with the size of the basis set, with errors ranging from +10 kJ mol^{-1} with the smallest 6-31+G(d,p) basis set considered to −2 kJ mol^{-1} with the largest 6-311++G(3d2f,2df,2p) basis set. These two basis sets were denoted DIDZ and MG3 by Zhao and Truhlar.[26] The trend suggests that an intermediate-sized basis set may give close accord with the experimental ΔH_0°, and accordingly, we focus on MPWB1K/6-31++G(2df,2p) results which give the best agreement with ΔH_0°. Corresponding geometries of stationary points are shown in Figure 3.

A molecule with a long (~2.4 × 10^{-10} m) two-center/three-electron Cl−N bond has been characterized previously, and our calculations are in general accord with those of McKee et al.[27] MPWB1K/6-31++G(2df,2p) geometries and frequencies imply that the equilibrium constant K_c for Cl−NH_3 formation at 290 K is 1.2 × 10^{-24} exp(BDE/RT) cm^3 molecule^{-1}, where BDE is the 0 K bond dissociation enthalpy. With a DFT value of 48 kJ mol^{-1}, $K_c \approx 5 \times 10^{-16}$ cm^3 molecule^{-1}, which implies that under the most favorable conditions (maximum [NH_3] and lowest T) up to two-thirds of the initial atomic Cl could be complexed by NH_3. Most of the room temperature runs would have a smaller fraction of Cl potentially complexed. The lack of observed p-dependence suggests that the two-center/three-electron species is not significantly formed in our experiments. The implication is that the BDE is probably slightly smaller than 48 kJ mol^{-1} and more in line with the ab initio values listed in Table 2. Lower-temperature experiments would check this proposition.

The potential energy diagram shown in Figure 4 reveals a TS with an energy below that of the final products, with an intervening complex bound by about 18 kJ mol^{-1} relative to NH_2 + HCl. The structure and energy of this complex are consistent with hydrogen bonding, and no barrier was found for dissociation to NH_2 + HCl. Energy optimizations starting with other Cl−H−N arrangements did not lead to new bound species. We now analyze this PES to derive rate constants for comparison with experiment, through consideration of the reverse process

$$NH_2 + HCl \rightarrow Cl + NH_3 \qquad (-1)$$

and then derive k_1 via microscopic reversibility: $k_1/k_{-1} = K_{eq}$ where the equilibrium constant was obtained from tabulated data[17] and the ΔH_0° derived above. This yields, to within 6%, $K_{eq} = 27.3T^{-0.049}$ exp(−2248/T) over 200−2000 K.

k_{-1} is derived via modified transition state theory (MTST). The standard TST result for the microcanonical rate constant is $k(E) = W^{\ddagger}(E^+)/h\rho_R(E)$,[28] where $\rho_R(E)$ is the density of states of the reactants at energy E, $W^{\ddagger}(E^+)$ is the total number of states of the TS with an energy below $E^+ = E - E_0$, counting from the ground state of the TS, and E_0 is the barrier height relative to the reactants. In the case where this

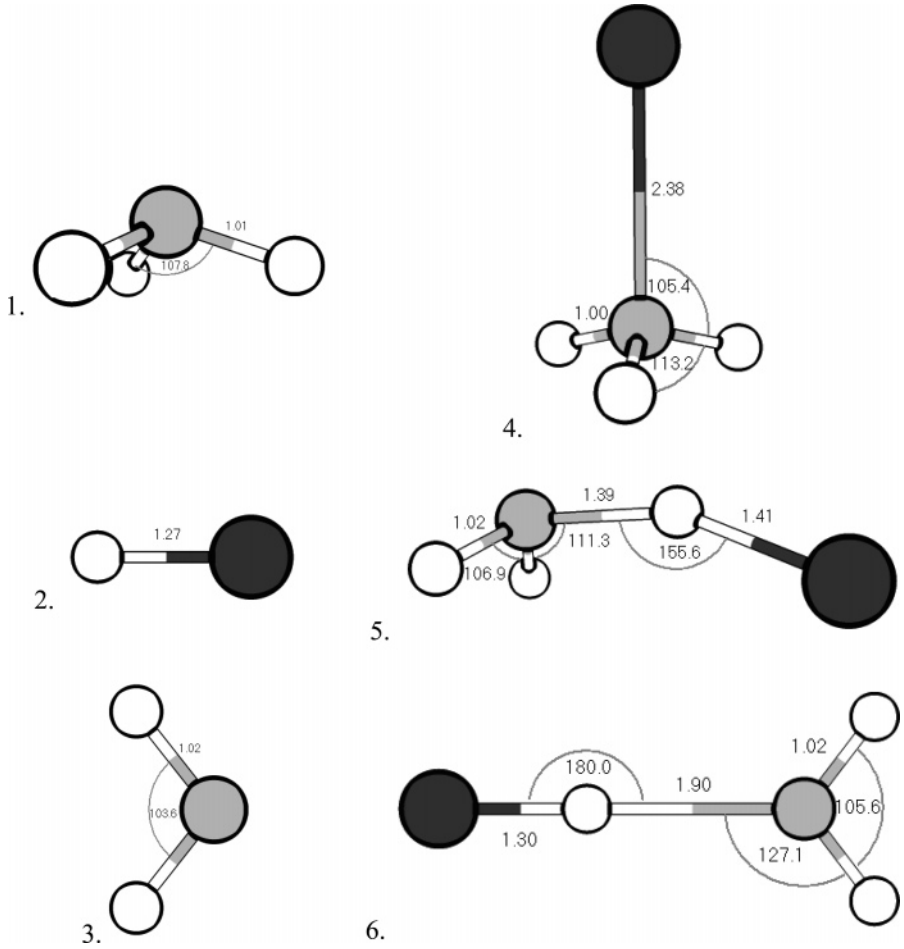

Figure 3. Geometries and frequencies (scaled by 0.955) of stationary points on the Cl + NH_3 potential energy surface, computed via MPWB1K/6-31++G(2df,2p) theory: 1. C_{3v} NH_3, 977, 1610 (2), 3440, 3576 (2) cm^{-1}. 2. HCl, 2932 cm^{-1}. 3. C_{2v} NH_2, 1475, 3332, 3427 cm^{-1}. 4. C_{3v} Cl−NH_3 adduct, 297, 342 (2), 817, 1570 (2), 3466, 3614 (2) cm^{-1}. 5. C_s transition state, 622i, 391, 400, 677, 984, 1180, 1502, 3376, 3481 cm^{-1}. 6. C_{2v} H_2N−HCl complex, 153, 156, 185, 556, 577, 1472, 2568, 3358, 3461 cm^{-1}.

barrier is positive, $k(E^+ < 0) = 0$, and thus

$$k(T) = \frac{1}{Q_R}\int_{E_0}^{\infty} \exp(-E/kT)\rho_R(E)k(E^+)\,dE$$

$$= \frac{kT}{h}\frac{\exp(-E_0/kT)}{Q_R}\int_0^{\infty} \rho^{\ddagger}(E^+)\exp(-E^+/kT)\,dE^+$$

$$= \frac{kT}{h}\frac{Q^{\ddagger}}{Q_R}\exp(-E_0/kT) \quad (5)$$

where $Q^{\ddagger}$ and Q_R are the partition functions for the TS and reactants, respectively. This is the usual TST result for $k(T)$.

For a reaction such as −1, where $E_0 < 0$, eq 5 is not applicable. At normal pressures, collisions are not rapid enough to thermalize the energy levels of the TS, and therefore, energy levels below the reactants are inaccessible (except in solution or at very high gas density). Thus, $E \geq 0$, and the lower bound of the first integration of eq 4 must be zero, which leads to

$$k(T) = \frac{1}{Q_R}\int_0^{\infty} \exp(-E/kT)\rho_R(E)k(E^+)\,dE$$

$$= \frac{kT\exp(-E_0/kT)}{hQ_R}\int_{-E_0}^{\infty} W^{\ddagger}(E^+)\exp(-E^+/kT)\frac{dE^+}{kT} \quad (6)$$

This result was noted by Garrett et al. in the context of improved canonical variational TST[29] and has recently been explored further by Krasnoperov et al.[30] They noted that the latter integral of eq 6 is smaller than $Q^{\ddagger}$ because the lower limit of integration is greater than zero, and so, $k(T)$ is reduced over the value derived via eq 5. Here, we also took into account angular momentum conservation (the J quantum number) and conservation of the energy of the K rotor at the TS, and quantum mechanical tunneling/reflection through the barrier. The latter effect is relatively small and only increases the rate constant by 9% at 300 K, 7% at 500 K, and 5% at 700 K. The interaction between NH_2 and HCl was calculated from a relaxed MPWB1K/

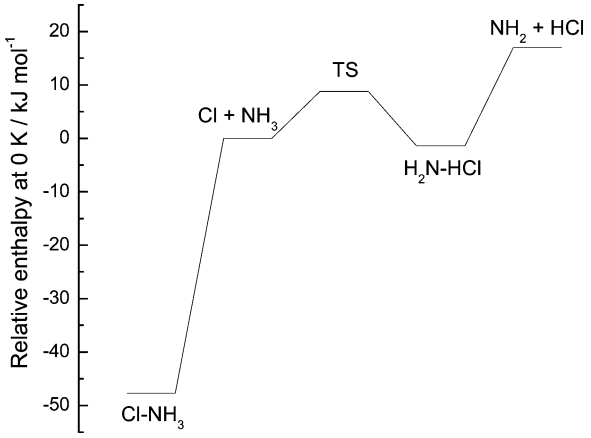

Figure 4. Potential energy diagram for Cl + NH_3 computed at the MPWB1K/6-31++G(2df,2p) level of theory.

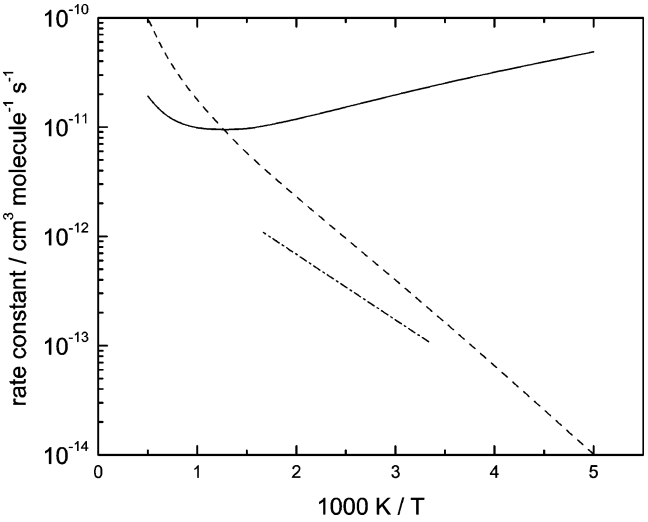

Figure 5. Comparison of theoretical and measured rate constants. Solid line, k_{-1}(MTST) for $NH_2 + HCl$; dashed line, k_1(MTST) for $Cl + NH_3$; dash−dot line, experimental k_1 for $Cl + NH_3$.

6-31++G(2df,2p) scan. This revealed that the energy dropped rapidly enough as the separation decreased for centrifugal barriers (at relevant J values) to be absent in the entrance valley leading to formation of the initial hydrogen-bonded intermediate, and thus, the reaction bottleneck is controlled by the TS. The full analytical expressions for this modified TST are given elsewhere.[30]

An Arrhenius plot of the computed k_{-1} is shown in Figure 5. Over 250−750 K, the theoretical rate constant is summarized by

$$k_{-1}(\mathrm{MTST}) = 4.08 \times 10^{-13}\, T^{0.343} \exp(+622/T)\ \mathrm{cm^3\ molecule^{-1}\ s^{-1}} \quad (7)$$

and clearly, the predicted temperature dependence is negative below 800 K. The deviation from the results of incorrect application of eq 5 is a factor of 3 at 298 K and increases with lower temperatures, so that the incorrectly derived k_{-1} would be too large and the temperature dependence too negative, as discussed by Krasnoperov et al.[30] There are no measurements of this $NH_2 + HCl$ reaction for direct comparison with eq 7.

Combination of k_{-1} with the equilibrium constant implies

$$k_1(\mathrm{MTST}) = 1.11 \times 10^{-11}\, T^{0.294} \exp(-1626/T)\ \mathrm{cm^3\ molecule^{-1}\ s^{-1}} \quad (8)$$

for $Cl + NH_3$ over 250−750 K. The agreement between k_1(MTST) and experiment is quite good, as seen in Figure 5, considering the exponential dependence on computed barrier height. The theoretically derived rate constant is around a factor of 3 too large. This might reflect an error in the barrier of a few kilojoules per mole, or the computed TS may be too tight. Nevertheless, the approximate magnitude and temperature dependence of k_1 are rationalized in terms of a TS whose energy lies below that of the final products (Figure 4). The role of hydrogen bonding between the products is to stabilize the TS, and details of the subsequent bound complex do not enter into the analysis.

5. Conclusions

The measured rate constant k_1 for $Cl + NH_3 \rightarrow NH_2 + HCl$ exhibits an activation energy more than 7 kJ mol^{-1} below the endothermicity. The reaction is therefore a clear counterexample to the common assumption that, for an endothermic process, $E_a \geq \Delta H°$. This result can be rationalized in terms of a PES based on density functional theory, where for the reverse process there is a bound complex in the entrance channel, followed by a transition state lying below the energy of $NH_2 + HCl$. Modified transition-state theory yields a negative temperature dependence for the $NH_2 + HCl$ reaction and, through microscopic reversibility, fair accord with k_1.

Acknowledgment. The UNT work was supported by the Robert A. Welch Foundation (grant B-1174), the National Science Foundation (grant CTS-0113605), and the UNT Faculty Research Fund. B.P.M. was supported through UNT's NSF Research Experience for Undergraduates program (grant CHE-0243795), and computer facilities were purchased with funding from the NSF (grant CHE-0342824).

References and Notes

(1) Daniels, F.; Alberty, R. A. *Physical Chemistry*, 2nd ed.; John Wiley: New York, 1961.

(2) Laidler, K. J.; Meiser, J. H. *Physical Chemistry*; Benjamin/Cummings: Menlo Park, CA, 1982.

(3) Fontijn, A.; Zellner, R. Influence of Temperature on Rate Coefficients of Bimolecular Reactions. In *Reactions of Small Transient Species*; Fontijn, A., Clyne, M. A. A., Eds.; Academic: New York, 1983.

(4) Russell, J. J.; Seetula, J. A.; Gutman, D. *J. Am. Chem. Soc.* **1988**, *110*, 3092.

(5) Kalinovski, I. J.; Gutman, D.; Krasnoperov, L. N.; Goumri, A.; Yuan, W.-J.; Marshall, P. *J. Phys. Chem.* **1994**, *98*, 9551.

(6) Nicovich, J. M.; Van Dijk, C. A.; Kreutter, K. D.; Wine, P. H. *J. Phys. Chem.* **1991**, *95*, 9890.

(7) Golden, D. M. *J. Phys. Chem.* **1979**, *83*, 108.

(8) Mozurkewich, M.; Benson, S. W. *J. Phys. Chem.* **1984**, *88*, 6429.

(9) McEwen, A. B.; Golden, D. M. *J. Mol. Struct.* **1990**, *224*, 357.

(10) Benson, S. W. *The Foundations of Chemical Kinetics*; McGraw-Hill: New York, 1960.

(11) Shi, Y.; Marshall, P. *J. Phys. Chem.* **1991**, *95*, 1654.

(12) Ding, L.; Marshall, P. *J. Phys. Chem.* **1992**, *96*, 2197.

(13) Okabe, H. *Photochemistry of Small Molecules*; Wiley: New York, 1978.

(14) Hanf, A.; Läuter, A.; Volpp, H.-R. *Chem. Phys. Lett.* **2003**, *368*, 445.

(15) Westenberg, A. A.; deHaas, N. *J. Chem. Phys.* **1977**, *67*, 2388.

(16) Mordaunt, D. H.; Dixon, R. N.; Ashfold, M. N. R. *J. Chem. Phys.* **1996**, *104*, 6472.

(17) *Thermodynamic Properties of Individual Substances*, 4th ed.; Gurvich, L. V., Veyts, I. V., Alcock, C. B., Eds.; Hemisphere: New York, 1989; Vol. 1.

(18) Bryukov, M. G.; Slagle, I. R.; Knyazev, V. D. *J. Phys. Chem. A* **2002**, *106*, 10532.

(19) *Thermodynamic Properties of Individual Substances*, 4th ed.; Gurvich, L. V.; Veyts, I. V.; Alcock, C. B., Eds.; Hemisphere: New York, 1992; Vol. 2.

(20) Litorja, M.; Ruscic, B. *J. Chem. Phys.* **1997**, *107*, 9852.

(21) Corchado, J. C.; Truhlar, D. G.; Espinosa-Garcia, J. *J. Chem. Phys.* **2000**, *112*, 9375.

(22) Russell, J. J.; Seetula, J. A.; Senkan, S. M.; Gutman, D. *Int. J. Chem. Kinet.* **1988**, *20*, 759.

(23) Frisch, M. J.; Trucks, G. W.; Schlegel, H. B.; Scuseria, G. E.; Robb, M. A.; Cheeseman, J. R.; Montgomery, J. A., Jr.; Vreven, T.; Kudin, K. N.; Burant, J. C.; Millam, J. M.; Iyengar, S. S.; Tomasi, J.; Barone, V.; Mennucci, B.; Cossi, M.; Scalmani, G.; Rega, N.; Petersson, G. A.; Nakatsuji, H.; Hada, M.; Ehara, M.; Toyota, K.; Fukuda, R.; Hasegawa, J.; Ishida, M.; Nakajima, T.; Honda, Y.; Kitao, O.; Nakai, H.; Klene, M.; Li, X.; Knox, J. E.; Hratchian, H. P.; Cross, J. B.; Bakken, V.; Adamo, C.; Jaramillo, J.; Gomperts, R.; Stratmann, R. E.; Yazyev, O.; Austin, A. J.; Cammi, R.; Pomelli, C.; Ochterski, J. W.; Ayala, P. Y.; Morokuma, K.; Voth, G. A.; Salvador, P.; Dannenberg, J. J.; Zakrzewski, V. G.; Dapprich, S.; Daniels, A. D.; Strain, M. C.; Farkas, O.; Malick, D. K.; Rabuck, A. D.; Raghavachari, K.; Foresman, J. B.; Ortiz, J. V.; Cui, Q.; Baboul, A. G.; Clifford, S.; Cioslowski, J.; Stefanov, B. B.; Liu, G.; Liashenko, A.; Piskorz, P.; Komaromi, I.; Martin, R. L.; Fox, D. J.; Keith, T.; Al-Laham,

M. A.; Peng, C. Y.; Nanayakkara, A.; Challacombe, M.; Gill, P. M. W.; Johnson, B.; Chen, W.; Wong, M. W.; Gonzalez, C.; Pople, J. A. *Gaussian 03*, revision C.02; Gaussian, Inc.: Wallingford, CT, 2004.

(24) Baboul, A. G.; Curtiss, L. A.; Redfern, P. C.; Raghavachari, K. *J. Chem. Phys.* **1999**, *110*, 7650.

(25) Montgomery, J. A., Jr.; Frisch, M. J.; Ochterski, J. W.; Petersson, G. A. *J. Chem. Phys.* **1999**, *110*, 2822.

(26) Zhao, Y.; Truhlar, D. G. *J. Phys. Chem. A* **2004**, *108*, 6908.

(27) McKee, M. L.; Nicolaides, A.; Radom, L. *J. Am. Chem. Soc*. **1996**, *118*, 8, 10571.

(28) Truhlar, D. G.; Garrett, B. C.; Klippenstein, S. J. *J. Phys. Chem.* **1996**, *100*, 12771.

(29) Garrett, B. C.; Truhlar, D. G.; Grev, R. S.; Magnuson, A. W. *J. Phys. Chem.* **1980**, *84*, 1730.

(30) Krasnoperov, L. N.; Peng, J.; Marshall, P. *J. Phys. Chem. A* **2006**, *110*, 3110.